

Synthesis of hexagonal-like ZnO/Ag composite with excellent photocatalytic activity

Ming Hua Wang, Hong Lan Cai , Zhen Liang Guo, Qing An Qiao, Shu Hua Ren, Dong Dong Zhu, Zhong Xin Xue

School of Chemistry and Material Science, Ludong University, Yantai, Shandong, 264025, People's Republic of China
✉ E-mail: honglancai@163.com

Published in *Micro & Nano Letters*; Received on 15th June 2018; Revised on 5th December 2018; Accepted on 3rd January 2019

Hexagonal-like zinc oxide (ZnO)/silver (Ag) composite was successfully synthesised by a flux/solvothermal route, and Ag nanoparticles are loaded on ZnO. Compared with pure ZnO, the attachment of Ag on ZnO can significantly increase visible-light absorption and reduce photoluminescence emission intensity. The photocatalytic performance of ZnO/Ag composite was evaluated by the degradation of Rhodamine B solution under ultraviolet (UV) light and visible light irradiation. The degradation rate of ZnO/Ag composite is obviously improved compared with pure ZnO and the commercial TiO₂ (P25) and is more than 2.5 and 2.9 times faster than that of pure ZnO under the UV and visible light irradiation, respectively. The enhanced photocatalytic activity of ZnO/Ag composite under UV irradiation was ascribed to the formation of Schottky barriers between Ag particles and ZnO. However, the superior photocatalytic activity under visible light irradiation could be attributed to the surface plasmon resonance of Ag particles.

1. Introduction: Wastewater from textile, paper, and some other industries contain residual dyes, which are not readily biodegradable. Adsorption and chemical coagulation are the two common techniques of treatment of such wastewater. However, these methods merely transfer dyes from the liquid to the solid phase causing secondary pollution and requiring further treatment [1–3]. Compared to these methods, semiconductor photocatalysis has been considered as a promising green technique for wastewater remediation because it can degrade organic pollutants in wastewater into CO₂ and H₂O with high efficiency [4–7]. At present, zinc oxide (ZnO) photocatalysts have been extensively investigated due to its low cost, non-toxicity, high photosensitivity and facile production [8–13]. However, the rapid recombination of photogenerated electron–hole pairs and the low utilisation of the solar light have become a principle factor that influences the photocatalytic efficiency of ZnO photocatalysts. One strategy to improve the photocatalytic efficiency is to modify ZnO particles with noble metals [14–17]. Among many noble metals, Ag is the cheapest noble metal and has potentials in industrial productions. Therefore, a series of ZnO/Ag nanocomposites with different morphologies have been prepared through various methods [18–25]. However, the design and preparation of photocatalysts with superior performance are still required. Herein, we reported the synthesis of the hexagonal-like ZnO/Ag composites by a two-step approach. The ultraviolet (UV) and visible-light photocatalytic performance of pure ZnO and ZnO/Ag composite was evaluated by using Rhodamine B (RhB) as a probe compound. The possible mechanism of photocatalysis was also discussed and proposed.

2. Experimental: Zinc nitrate hexahydrate (Zn(NO₃)₂·6H₂O), urea (CO(NH₂)₂), silver nitrate (AgNO₃), methanol and ethanol were of analytical grade and directly used without any purification. Commercial TiO₂ (P25) was used as reference photocatalyst and was employed as received. Deionised water was employed throughout experiments.

ZnO/Ag composites were synthesised via a two-step route. At the first step, hexagonal-like ZnO particles were synthesised by a simple reflux method. 13.38 g Zn(NO₃)₂·6H₂O and 10.80 g urea were dissolved in 150 ml deionised water. After being stirred for 10 min, the solution was aged in a flask at 95°C for 2.5 h. After naturally cooling down to room temperature, the resulting precipitates were collected by centrifugation, washed three times with ethanol

and distilled water, respectively, and then dried at 70°C in air for 6 h. The final white ZnO powders were obtained through a heat treatment of the precursors at 500°C in air for 2 h. At the second step, ZnO/Ag composites were prepared by a solvothermal method [18]. 0.1 g ZnO powders were added into 30 ml methanol containing 0.0105 g AgNO₃ (the nominal mass ratio of Ag to ZnO is 6.7%) and ultrasonically dispersed for 10 min. The suspension solution was maintained at 100°C for 4 h in a 50 ml Teflon-lined autoclave. After the autoclave was being cooled down to room temperature, the resulting products were collected by centrifugation, washed with water/ethanol, and finally dried at 70°C for 12 h.

The phase and crystallinity of the samples were characterised by X-ray diffraction (XRD) (*D/max* 2500, Japan). The morphology and dimension of the samples were characterised by using a transmission electron microscope (TEM) (JEM-1230, JEOL, Japan). UV–visible (UV–vis) absorption spectra of the samples were recorded on a UV–vis spectrophotometer (UV-2550, Shimadzu, Japan). Photoluminescence (PL) spectra were measured on an LS55 fluorescence spectrometer using a Xenon lamp as the excitation source. The actual content of noble metal Ag deposited in ZnO/Ag composite was measured by inductive coupled plasma optical emission spectrometry (ICP-OES) (ICPE-9000, Shimadzu, Japan).

The photocatalytic performance of ZnO/Ag composite was evaluated by using RhB as a dye pollutant. A high pressure Hg UV lamp (300 W) with a maximum emission at 365 nm was served as the UV light source. A 300 W Xenon lamp (CEL-HXF300) was used as the visible light source with a 400 nm cut-off filter. In a typical procedure, 30 mg catalyst (P25, ZnO or ZnO/Ag) was dispersed into 50 ml aqueous solution of RhB (1.5×10^{-5} mol l⁻¹). After stirring in the dark for 0.5 h, the suspensions were placed under light irradiation. During the photoreaction, the samples were collected at regular intervals and centrifuged to remove the catalyst. The concentration of RhB solution before and after degradation was measured by using a UV–vis spectrometer. Total organic carbon (TOC) was followed by means of a TOC analyser (TOC-VCPH, Shimadzu, Japan). Mineralisation degree (%) was evaluated by the TOC values upon 50 min of UV illumination using the formula $[1 - (\text{final TOC})/(\text{initial TOC})] \times 100$.

3. Results and discussion: The crystal phase of pure ZnO and ZnO/Ag composite was characterised by XRD. As shown in Fig. 1, all of the diffraction peaks can be indexed to the hexagonal

ZnO (marked with *, JCPDS Card No. 36-1451). For the XRD pattern of ZnO/Ag composite, the other two diffraction peaks at 38.22 and 44.36 can be attributed to the (111) and (200) crystal

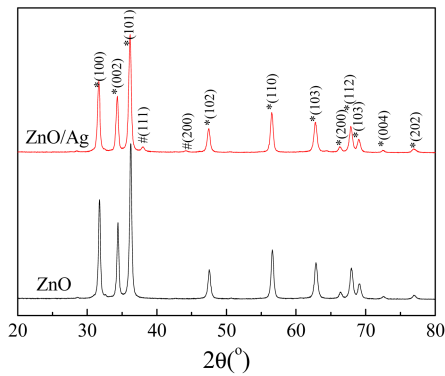


Fig. 1 XRD patterns of pure ZnO and ZnO/Ag composite

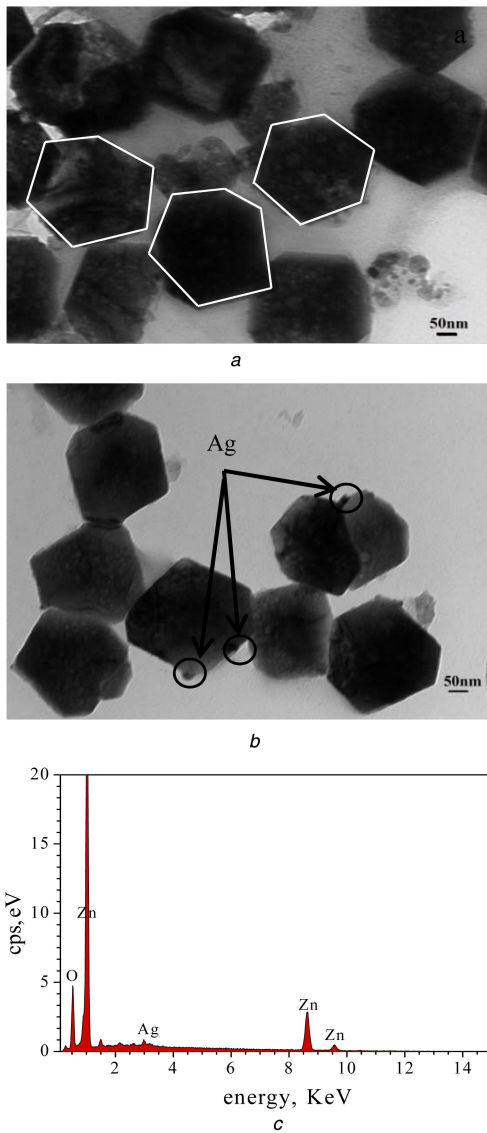


Fig. 2 TEM image of pure ZnO, TEM and EDS spectrum of ZnO/Ag composite
a TEM image of pure ZnO
b TEM image of ZnO/Ag composite
c EDS spectrum of ZnO/Ag composite

planes of cubic phase of Ag (marked with #, JCPDS Card No. 04-0783). Therefore, ZnO/Ag composite is prepared by a facile sol-thermal method.

The morphology and size of the obtained ZnO and ZnO/Ag composite were explored by TEM. Fig. 2a shows a typical TEM image of pure ZnO, showing that ZnO is mainly composed of many monodisperse, hexagonal-like shape particles with the diameter in the range of 150–200 nm. After the incorporation of Ag, as shown in Fig. 2b, ZnO/Ag composite maintains hexagonal-like morphology, indicating that the morphology of ZnO is almost unaltered after the deposition of Ag. Nevertheless, the ZnO/Ag surface is dissimilar from the pure ZnO surface, a tiny number of particles are found on the ZnO surface. The energy dispersive X-ray spectroscopy (EDS) spectrum of ZnO/Ag composite is shown in Fig. 2c. The elements Ag, Zn, and O are observed in the spectra. These results demonstrate that the tiny particles on the ZnO surface are Ag nanoparticles. The ICP-OES result indicates that the real Ag content in the ZnO/Ag is 1.3 wt%, which was much lower than the nominal content (6.7 wt%).

Fig. 3 shows UV–vis absorption spectra of pure ZnO and ZnO/Ag composite. Pure ZnO exhibits obvious UV absorption peak at 372 nm, which can be assigned to free excitonic absorption of the particles [19]. Compared with that of pure ZnO, another broad absorption peak centred at 450 nm can be found from the UV–vis absorption spectrum of the ZnO/Ag composite. The absorption is attributed to the characteristic absorption of surface plasmon resulting from the metallic Ag [20]. The appearance of two kinds of characteristic absorption bands further confirms that the as-synthesised samples are composed of Ag and ZnO.

Fig. 4 shows the PL spectra of pure ZnO and ZnO/Ag composite excited with a light of 325 nm wavelength. The two samples reveal similar emission spectra. A UV emission band centred at ~390 nm is attributed to the UV emission of the ZnO particles [21], while several emission bands from 400 to 500 nm are ascribed to the charge carrier relaxation through surface-related trap states [22].

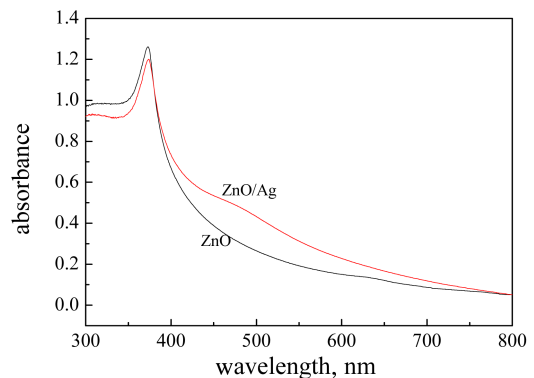


Fig. 3 UV–vis absorption spectra of pure ZnO and ZnO/Ag composite

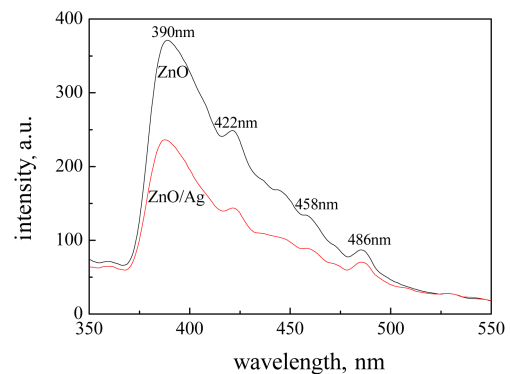


Fig. 4 PL spectra of pure ZnO and ZnO/Ag composite

Attachment of Ag particle to the ZnO obviously reduces the intensity of UV emission peak, indicating Ag particles can increase the separation of photoexcited charge carrier and inhibit the recombination of electron-hole pairs, and thus be importantly favourable for the improvement of the photocatalytic activity of ZnO [23].

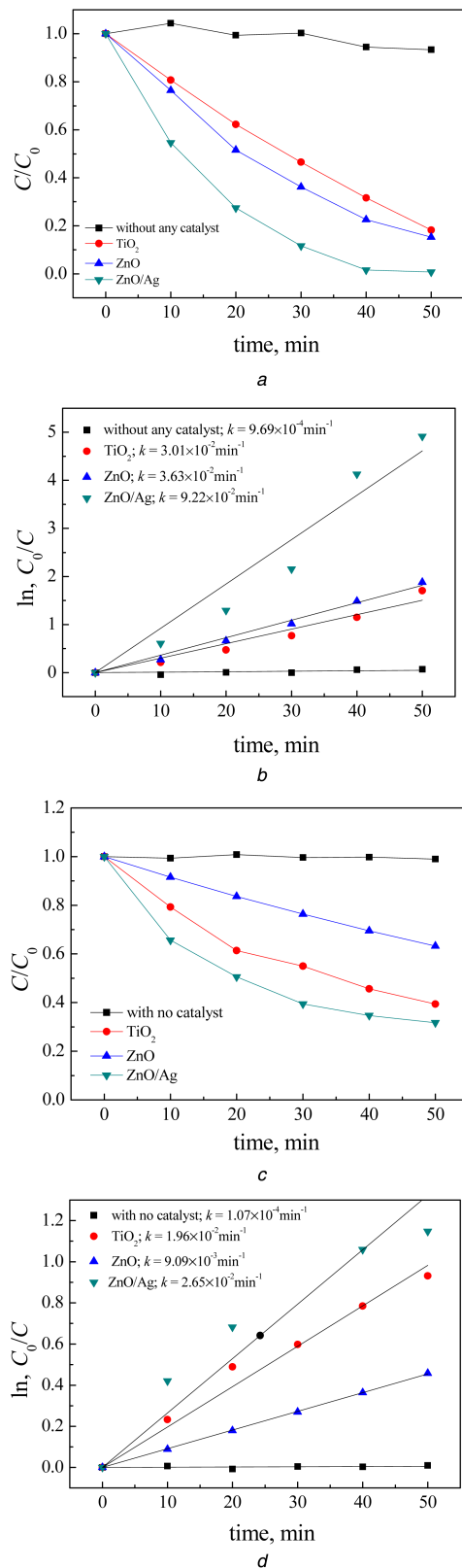


Fig. 5 Photocatalytic activity and kinetics of the P25, pure ZnO and ZnO/Ag composite for degradation of RhB under a, b UV c, d Visible light irradiation

The photocatalytic performance of ZnO/Ag composite was evaluated by taking RhB as the target dye pollutant under UV and visible light irradiation. Fig. 5a shows the degradation rate of RhB under UV irradiation in the presence of different photocatalysts (ZnO, ZnO/Ag, and P25), where C_0 and C are the initial concentration of RhB and concentration of RhB at time t , respectively. The concentration of RhB has no obvious change in the absence of a photocatalyst. The photodegradation efficiency of RhB was about 82, 85 and 99% for P25, ZnO, and ZnO/Ag composite, respectively, when the reaction was performed under UV light irradiation for 50 min. It can be seen that ZnO/Ag composite exhibits a much higher photocatalytic activity than that of pure ZnO and TiO_2 for photodegradation of the RhB. The catalytic activity of ZnO is slightly higher than that of P25. Final mineralisation degrees were calculated from the TOC measurements and values (data not shown) for P25, ZnO, and ZnO/Ag composite are 80, 82, and 92%, respectively. The photodegradation of RhB can be considered as a pseudo-first-order reaction, the rate expression is given by the equation: $\ln(C_0/C) = kt$ [24]. The variation in $\ln(C_0/C)$ as a function of irradiation time was given in Fig. 5b. The apparent rate constant k was determined by linear fitting for different samples. Compared with P25 and pure ZnO, the ZnO/Ag composite displayed the highest photocatalytic activity with a rate constant ($k = 9.22 \times 10^{-2} \text{ min}^{-1}$), i.e. 2.5 times as large as that of pure ZnO ($k = 3.63 \times 10^{-2} \text{ min}^{-1}$). These results show that the photocatalytic activity of ZnO can be obviously improved in the presence of Ag particles.

Figs. 5c and d show the photocatalytic activity and kinetics of the P25, pure ZnO, and ZnO/Ag composite for degradation of RhB under visible-light irradiation, respectively. It is found that the degradation rate of RhB is only 36% pure ZnO under visible-light irradiation for 50 min, while degradation rate reaches 60 and 68% when the TiO_2 and ZnO/Ag composite was used, respectively. It is well known that ZnO and TiO_2 have no absorption in the visible region. The degradation of RhB with P25 or ZnO under the visible irradiation is associated with a photosensitising effect exerted by the RhB [25, 26]. However, ZnO/Ag composite exhibits much higher photocatalytic performance, of which k ($2.65 \times 10^{-2} \text{ min}^{-1}$) was 2.9 times larger than that pure ZnO ($k = 9.09 \times 10^{-3} \text{ min}^{-1}$), which may be attributed to the presence of Ag particles in ZnO [27].

Good recycling stability is a very important parameter for photocatalysts in the practical application. Stability tests were performed by using ZnO/Ag to degrade RhB in four repeated cycles. Fig. 6 shows the degradation percentages of RhB aqueous solution after 50 min of UV-illumination for four cycles. The obtained degradation percentages are 99.4, 98.5, 94.2, and 92.4%, respectively, which indicates that ZnO/Ag exhibits effective photo stability with a slight decrement in their photocatalytic activity.

The enhanced photocatalytic mechanism of ZnO/Ag under UV and visible light irradiation could be illustrated in Fig. 7. Under UV light irradiation, when photon energy is higher than or equal

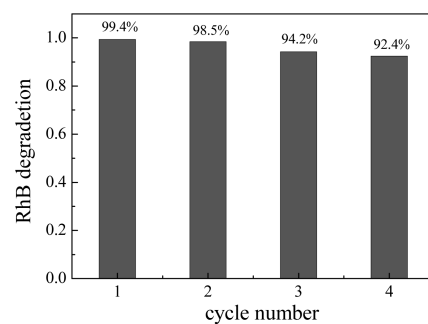


Fig. 6 Four repeated processes by using ZnO/Ag to degrade RhB after 50 min of UV illumination

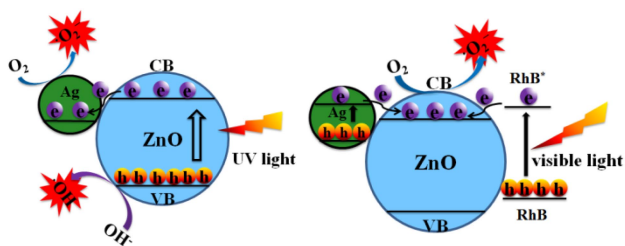


Fig. 7 Schematic diagram to process of photosensitized degradation of RhB by ZnO/Ag composite under UV and visible light irradiation

to the band gap of ZnO crystals, electrons (e^-) in the valence band (VB) will be excited to the conduction band (CB) and generate the same amount of holes (h^+) in the VB. The photoelectron can be easily transferred to Ag particles. Therefore, Ag particles, acting as electron sinks, reduce the recombination of photo-induced electrons and holes, and prolong the lifetime of the electron pairs. Subsequently, the electrons can be trapped by the adsorbed O_2 molecules, and further converted into a superoxide radical anion ($\bullet O_2^-$) [28]. At the same time, the photo-induced holes in ZnO can be also readily trapped by surface H_2O molecules to generate $\bullet OH$ radicals. RhB molecules can be degraded into CO_2 and H_2O by the action of $\bullet O_2^-$ and $\bullet OH$ radicals [29]. For the photocatalysis under visible-light irradiation, on the one hand, the adsorbed RhB would be photoactivated by the visible light, followed by electron transfer from the excited RhB (RhB^*) to the

CB of ZnO, which separated the $RhB^{\bullet+}$ and electron, preventing the recombination process [30–32]. On the other hand, due to the surface plasma resonance of Ag particles, electron-hole pairs are photo-generated in the Ag particles under visible-light irradiation. The electron is able to transfer from Ag to CB of ZnO [33]. The separated electrons might then be consumed by the oxygen molecules dissolved in the solution to generate various reactive oxidative species, thus promoting the photocatalysis.

4. Conclusion: In summary, hexagonal-like ZnO/Ag composite was synthesised via a flux/solvothermal route. Compared with pure ZnO and P25, ZnO/Ag composites had shown significant enhanced photocatalytic activity for RhB solution under UV and visible light irradiation. The enhanced photocatalytic activity could be attributed to the decorated Ag particles. The Ag particles deposited on the ZnO surface act as the electron sinks to improve the charge separation in UV irradiation, while the plasmatic effect of the deposited Ag particles enhances the photocatalytic activity in the visible region. Moreover, ZnO/Ag composite can exhibit good photocatalytic activity after four cycles.

5. Acknowledgments: This work was supported by the Nature Science Foundation of China (grant no. 21501087), the Industry, Education, and Research Cooperative Education Project of Ministry of Education of China (grant no. 201702068013) and the Nature Science Foundation of Shandong Province of China (grant no. ZR2014BM037).

6 References

- Zhang S.X., Zhang Y.Y., Bi G.M., *ET AL.*: ‘Mussel-inspired polydopamine biopolymer decorated with magnetic nanoparticles for multiple pollutants removal’, *J. Hazard. Mater.* 2014, **270**, pp. 27–34
- Guo L., Cao Y.C., Li G.Y., *ET AL.*: ‘Preparation of starch sulfate resin and its adsorption performance for malachite green’, *Desalin. Water Treat.*, 2017, **97**, pp. 321–328
- Zhang Z.J., Zhu L.L., Meng Y.L., *ET AL.*: ‘Adsorption of methylene blue from aqueous solution by sol-gel silica doped with sec-octylphenoxyl acetic acid’, *Desalin. Water Treat.*, 2018, **108**, pp. 338–344
- Zhou L., Wang L.Z., Lei J.Y., *ET AL.*: ‘Fabrication of $TiO_2/Co-g-C_3N_4$ heterojunction catalyst and its photocatalytic performance’, *Catal. Commun.*, 2017, **89**, pp. 125–128
- Reddy C.V., Babu B., Shim J.: ‘Synthesis, optical properties and efficient photocatalytic activity of CdO/ZnO hybrid nanocomposite’, *J. Phys. Chem. Solids*, 2018, **112**, pp. 20–28
- Li Y.F., Jin R.X., Fang X.: ‘In situ loading of Ag_2WO_4 on ultrathin $g-C_3N_4$ nanosheets with highly enhanced photocatalytic performance’, *J. Hazard. Mater.*, 2016, **313**, pp. 219–228
- Strbac D., Aggelopoulos C.A., Strbac G.: ‘Photocatalytic degradation of naproxen and methylene blue: comparison between ZnO, TiO_2 and their mixture’, *Proc. Saf. Environ.*, 2018, **113**, pp. 174–183
- Lei A.H., Qu B.H., Zhou W.C., *ET AL.*: ‘Facile synthesis and enhanced photocatalytic activity of hierarchical porous ZnO microspheres’, *Mater. Lett.*, 2012, **66**, pp. 72–75
- Wu H.Y., Xie Q.S., An L., *ET AL.*: ‘Facile preparation of porous flower-like ZnO microspheres with excellent photocatalytic performance’, *Mater. Lett.*, 2015, **139**, pp. 393–396
- Wang Y.X., Yang Y.Q., Xi L.M., *ET AL.*: ‘A simple hydrothermal synthesis of flower-like ZnO microspheres and their improve photocatalytic activity’, *Mater. Lett.*, 2016, **180**, pp. 55–58
- Song R.Q., Xu A.W., Deng B., *ET AL.*: ‘From layered basic zinc acetate nanobelts to hierarchical zinc oxide nanostructures and porous zinc oxide nanobelts’, *Adv. Funct. Mater.*, 2007, **17**, pp. 296–306
- Liu J.P., Huang X.T., Li Y.Y., *ET AL.*: ‘Large-scale synthesis of flower-like ZnO structures by a surfactant-free and low-temperature process’, *Mater. Chem. Phys.*, 2006, **98**, pp. 523–527
- Cho S.H., Jung S.H., Lee K.H.: ‘Morphology-controlled growth of ZnO nanostructures using microwave irradiation: from basic to complex structures’, *J. Phys. Chem. C*, 2008, **112**, pp. 12769–12776
- Qu X., Yang R., Tong F., *ET AL.*: ‘Hierarchical ZnO microstructures decorated with Au nanoparticles for enhanced gas sensing and photocatalytic properties’, *Powder Technol.*, 2018, **330**, pp. 259–263
- Fernandez L.M., Fernandez A.S., Milošević O., *ET AL.*: ‘Solvothermal synthesis of Ag/ZnO and Pt/ZnO nanocomposites and comparison of their photocatalytic behaviors on dyes degradation’, *Adv. Powder Technol.*, 2016, **27**, pp. 983–993
- Zhong J.B., Li J.Z., He X.Y., *ET AL.*: ‘Improved photocatalytic performance of Pd-doped ZnO’, *Curr. Appl. Phys.*, 2012, **12**, pp. 998–1001
- Liu Y.J., Xu C.X., Zhu Z., *ET AL.*: ‘Self-assembled ZnO/Ag hollow spheres for effective photocatalysis and bacteriostasis’, *Mater. Res. Bull.*, 2018, **98**, pp. 64–69
- Zhang L.L., Zhu D., He H.X., *ET AL.*: ‘Enhanced piezo/solar-photocatalytic activity of Ag/ZnO nano-tetrapods arising from the coupling of surface plasmon resonance and piezophototronic effect’, *J. Phys. Chem. Solids*, 2017, **102**, pp. 27–33
- Raula M., Rashid M.H., Paira T.K., *ET AL.*: ‘Ascorbate-assisted growth of hierarchical ZnO nanostructures: sphere, spindle, and flower and their catalytic properties’, *Langmuir*, 2010, **26**, (11), pp. 8769–8782
- Guo X.H., Ma J.Q., Ge H.G., *ET AL.*: ‘Preparation, characterization, and photocatalytic performance of pear-shaped ZnO/Ag core-shell submicrospheres’, *J. Phys. Chem. Solids*, 2013, **74**, pp. 784–788
- Patil S.S., Mali M.G., Tamboli M.S., *ET AL.*: ‘Green approach for hierarchical nanostructured Ag-ZnO and their photocatalytic performance under sunlight’, *Catal. Today*, 2016, **260**, pp. 126–134
- Zhang X.D., Wang Y.X., Hou F.L., *ET AL.*: ‘Effects of Ag loading on structural and photocatalytic properties of flower-like ZnO microspheres’, *Appl. Surf. Sci.*, 2017, **391**, pp. 476–483
- Wang M., Xu J.Y., Sun T.M., *ET AL.*: ‘Facile photochemical synthesis of hierarchical cake-like ZnO/Ag composites with enhanced visible-light photocatalytic activities’, *Mater. Lett.*, 2018, **219**, pp. 236–239
- Hong Y., Tian C.G., Jiang B.J., *ET AL.*: ‘Facile synthesis of sheet-like ZnO assembly composed of small ZnO particles for highly efficient photocatalysis’, *J. Mater. Chem. A*, 2013, **1**, pp. 5700–5708
- Jaramillo-Páez C., Navío J.A., Hidalgo M.C.: ‘Silver-modified ZnO highly UV-photoactive’, *J. Photochem. Photobiol. A*, 2018, **356**, pp. 112–122
- Murcia-López S., Hidalgo M.C., Navío J.A.: ‘Degradation of rhodamine B/phenol mixtures in water by sun-like excitation of a $Bi_2WO_6-TiO_2$ photocatalyst’, *Photochem. Photobiol.*, 2013, **89**, pp. 832–840
- Liang Y.M., Guo N., Li L.L., *ET AL.*: ‘Fabrication of porous 3D flower-like Ag/ZnO heterostructure composites with enhanced photocatalytic performance’, *Appl. Surf. Sci.*, 2015, **332**, pp. 32–39

- [28] Kadam A.N., Bhopate D.P., Kondalkar V.V.: 'Facile synthesis of Ag-ZnO core-shell nanostructures with enhanced photocatalytic activity', *J. Ind. Eng. Chem.*, 2018, **61**, pp. 78–86
- [29] Saravanakumar K., Muthuraj V., Jeyaraj M.: 'The design of novel visible light driven Ag/CdO as smart nanocomposite for photo-degradation of different dye contaminants', *Spectrochim. Acta A*, 2018, **188**, pp. 291–300
- [30] Deng Q., Duan X.W., Dickon H.L.N., *ET AL.*: 'Ag nanoparticle decorated nanoporous ZnO microrods and their enhanced photocatalytic activities', *ACS Appl. Mater. Interfaces*, 2012, **4**, pp. 6030–6037
- [31] Akir S., Barras A., Coffinier Y., *ET AL.*: 'Eco-friendly synthesis of ZnO nanoparticles with different morphologies and their visible light photocatalytic performance for the degradation of rhodamine B', *Ceram. Int.*, 2016, **42**, pp. 10259–10265
- [32] Liu H.R., Hu Y.C., Zhang Z.X., *ET AL.*: 'Synthesis of spherical Ag/ZnO heterostructural composites with excellent photocatalytic activity under visible light and UV irradiation', *Appl. Surf. Sci.*, 2015, **355**, pp. 644–652
- [33] Yang C., Li Q.S.: 'ZnO inverse opals with deposited Ag nanoparticles: fabrication, characterization and photocatalytic activity under visible light irradiation', *J. Photochem. Photobiol. A*, 2019, **371**, pp. 118–127